

Aromatic Thiol pK_a Effects on the Folding Rate of a Disulfide Containing Protein[†]

Jonathan D. Gough, Joseph M. Gargano, Anthony E. Donofrio, and Watson J. Lees*

Department of Chemistry, Syracuse University, Syracuse, New York 13244

Received February 24, 2003; Revised Manuscript Received August 7, 2003

ABSTRACT: The production of proteins via recombinant DNA technology often requires the in vitro folding of inclusion bodies, which are protein aggregates. To create a more efficient redox buffer for the in vitro folding of disulfide containing proteins, aromatic thiols were investigated for their ability to increase the folding rate of scrambled RNase A. Scrambled RNase A is fully oxidized RNase A with a relatively random distribution of disulfide bonds. The importance of the thiol pK_a value was investigated by the analysis of five *para*-substituted aromatic thiols with pK_a values ranging from 5.2 to 6.6. Folding was measured at pH 6.0 where the pK_a value of the thiols would be higher, lower, or equal to the solution pH. Thus, relative concentrations of thiol and thiolate would vary across the series. At pH 6.0, the aromatic thiols increased the folding rate of RNase A by a factor of 10–23 over that observed for glutathione, the standard additive. Under optimal conditions, the apparent rate constant increased as the thiol pK_a value decreased. Optimal conditions occurred when the concentration of protonated thiol in solution was approximately 2 mM, although the total thiol concentration varied considerably. The importance of the concentration of protonated thiol in solution can be understood based on equilibrium effects. Kinetic studies suggest that the redox buffer participates as the nucleophile and/or the center thiol in the key rate determining thiol disulfide interchange reactions that occur during protein folding. Aromatic thiols proved to be kinetically faster and more versatile than classical aliphatic thiol redox buffers.

Native disulfide bonds are essential for the function of numerous extracellular proteins and almost all therapeutic proteins (1, 2). During the production of recombinant proteins, native disulfide bonds can be formed either in vivo or in vitro (3–5). The in vivo overexpression of proteins often results in the formation of aggregates of misfolded proteins, also known as inclusion bodies (3, 6–8). The formation of inclusion bodies simplifies protein purification but necessitates resolubilization followed by in vitro protein folding (5, 8, 9). In general, the slow step during in vitro folding of disulfide containing proteins is the formation of native disulfide bonds via thiol disulfide interchange reactions. To increase the rate determining steps, a mixture of a small molecule aliphatic thiol and a disulfide is introduced (3, 5).

The in vitro folding rate of disulfide containing proteins has been increased by the addition of protein catalysts and a limited number of small molecule thiols (10–15). The in vitro use of protein catalysts, such as protein disulfide isomerase (PDI),¹ significantly increases the rate of protein folding but is impractical due to their high cost and low catalytic activity (11). Small molecules, although slower, are less expensive and subsequently easier to remove from the native protein. Standard additives are aliphatic thiols such as mercaptoethanol, glutathione (GSH), cysteine, and dithiothreitol (DTT) (12, 15). More recently the usefulness of the

dithiol (\pm)-*trans*-1,2-bis(2-mercaptoacetamido)cyclohexane (BMC) and 4-mercaptobenzeneacetate, an aromatic thiol, has been demonstrated by Raines et al. and us, respectively. The aliphatic dithiol BMC increases the yield of native protein relative to standard additives but not the rate constant for protein folding (10, 13). However, the aromatic thiol increases the rate constant of protein folding by a factor of 6 or 5 over glutathione at pH 7.0 and 7.7, respectively (14). Very few other small molecule thiols have been investigated for their protein folding capabilities.

The folding pathways of a number of disulfide containing proteins have been extensively studied (16–20). Each of these pathways entails multiple thiol disulfide interchange reactions between the protein and the small molecule thiols and disulfides. The mechanism of a thiol disulfide interchange reaction involves a nucleophilic attack of a thiolate on a disulfide, Figure 1 (21, 22). The rate of the thiol

[†] This work was supported by the National Science Foundation (Grant Number CHE 9975076).

* To whom correspondence should be addressed. Present address: Department of Chemistry and Biochemistry, Florida International University, University Park Campus, 11200 SW 8th Street, Miami, FL 33199. Telephone: 305-348-3993. Fax: 305-348-3772. E-mail: leeswj@fiu.edu.

¹ Abbreviations: 1S, RNase A with one disulfide bond; 2S, RNase A with two disulfide bonds; 2-PDE, 2-pyridyldithioethanol; 3S, RNase A with three disulfide bonds; 4S, RNase A with four disulfide bonds; AcOH, acetic acid; AEMTS, 2-aminoethyl methanethiosulfonate; ArSH, aromatic thiol; ArSSAr, aromatic disulfide; ArSX, aromatic species; Bis-tris, bis[2-hydroxyethyl]iminotris[hydroxymethyl]methane; BMC, dithiol (\pm)-*trans*-1,2-bis(2-mercaptoacetamido)cyclohexane; CbzCl, benzyl chloroformate; cCMP, cytidine 2',3' – cyclic monophosphate; DMF, dimethyl formamide; DTT, dithiothreitol; EDTA, ethylenediaminetetraacetic acid; EtOAc, ethyl acetate; EtOH, ethyl alcohol; GSH, glutathione; GSSG, glutathione disulfide; GSX, glutathione species; MeOH, methanol; N, native protein; PDI, protein disulfide isomerase; PSH, protein thiol; PSSP, protein disulfide; PSSR, mixed disulfide; R, fully reduced protein; RNase A, ribonuclease A; R–S[–]_{nuc}, nucleophilic thiolate; R–S_c, center thiol; R–S_{lg}, leaving group thiol; RSH, small molecule thiol; RSSR, small molecule disulfide; SH, thiol in the protonated form; sRNase A, scrambled ribonuclease A.

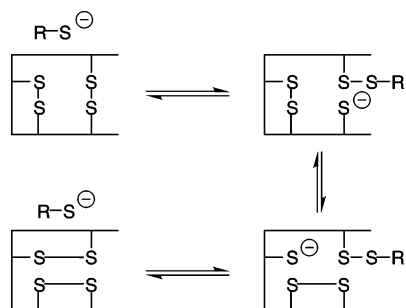


FIGURE 1: The thiol disulfide interchange reactions of a small molecule thiolate (RS^-) and a protein disulfide. The small molecule thiol first acts as a nucleophile and ultimately as a leaving group.

disulfide interchange reaction is dependent on the concentration of the thiolate and disulfide. The concentration of the thiolate is a function of the total thiol concentration, the thiol pK_a , and the solution pH.

We sought to gain insight into how aromatic thiols effect the thiol disulfide interchange reactions that occur during the protein folding process and to improve the effectiveness of aromatic thiols for protein folding. In doing so, it was important to understand how the pK_a value of the aromatic thiol affected the protein folding rate constant. In addition by changing the thiol pK_a value at a given pH, the relative concentration of thiol (protonated) and thiolate (deprotonated) varied. The roles of the thiol and thiolate in protein folding reactions were discerned. Practically, it was important to find the optimal aromatic thiol for folding proteins at a given pH. Herein, a series of aromatic thiols, with a range of thiol pK_a values, were evaluated for their protein folding capabilities.

MATERIALS AND METHODS

General Information. NMR chemical shifts were internally referenced to the solvent. All reagents purchased were used without purification. E & R Microanalytical Laboratory Inc. (Parsippany, NJ) performed all elemental analyses. Mass spectra were obtained by the Mass Spectroscopy Laboratory at the University of Illinois at Urbana-Champaign. RNase A was purchased from Sigma. Compound **1** was obtained from Toronto Research Corporation or synthesized (23, 24). Compounds **2**, **3** (24), and **4** (25) were synthesized as previously described. Scrambled RNase A (0.27 mM) (26, 27), RNase A with approximately a random distribution of disulfide bonds, was stored at -5°C in an aqueous solution (0.6% AcOH, 1 mM EDTA). All buffers used for protein folding were prepared by the addition of Bis-tris (bis[2-hydroxyethyl]iminotris[hydroxymethyl]methane) to a 0.6% solution of AcOH. The protein folding buffers contained 1 mM EDTA. Solutions were deoxygenated by bubbling Ar through them for 30 min.

Protein Folding (28, 29). Refolding experiments were conducted at 25°C . Protein aliquots were adjusted to pH 6.0 by the addition of 0.1 M base (Bis-tris). Stock solutions of 10 mM glutathione (GSH), 5 mM glutathione disulfide (GSSG), and 10–30 mM of aromatic thiol (ArSH-1-6) were prepared individually in deoxygenated buffer (Bis-tris/EDTA) and deoxygenated for use in the refolding reactions. The refolding reaction was initiated by the addition of the

pH-adjusted sRNase A. The refolding reaction (total volume 500 μL) contained sRNase A (25 μM), GSSG (0.2 mM), varying amounts of aromatic thiol (ArSH-1-6) or glutathione (GSH), and buffer (pH 6.0 – bis-tris/EDTA). Aliquots were withdrawn at specific times and assayed for enzymatic activity. The protein was allowed to refold until no further increase in activity was observed (up to 2 days).

Enzymatic Assay. The concentration of active protein was determined by the assay for native RNase A (14). For the assays of compounds **3-5**, 10 μL of a 0.5 M 2-aminoethyl methanethiosulfonate (AEMTS) solution was added to the cuvette containing the pH 5.0 buffer, before the protein solution was added, to reduce the background absorbance due to the aromatic thiolate.

Folding Rate. The folding rate was determined by plotting the concentration of active protein versus time. The concentration of active protein was expressed as % refolded, where % refolded = $([\text{active protein}]/(2.5 \times 10^{-5} \text{ M}))100\%$. The plot was fit using least squares to % refolded = $A(1 - e^{-kt})$, where A is maximum % activity achieved, k is the refolding rate constant, and t is time in minutes. The value of Ak corresponds to the initial rate of protein folding. For a given thiol, the maximum Ak value represents the optimal folding conditions.

Equilibrium Determination. The equilibrium constants for compounds **1** and **4** with glutathione were determined at pD 6 and 4, respectively, in D_2O using ^1H NMR. At these pD values, almost all of the aromatic thiol will be in the protonated form, since thiol pK_a values increase by approximately 0.5 in buffered D_2O (30). Solutions containing 1–10 mM thiol and 1–5 mM disulfide were prepared in D_2O ($\text{D}_3\text{PO}_4/\text{NaOD}/\text{D}_3\text{CCOOD}$) at the appropriate pD. Equilibrium was approached from both directions. Integration of the component peaks gave the relative concentrations of the five components (aromatic thiol, aromatic disulfide, glutathione, glutathione disulfide, and mixed aromatic-glutathione disulfide). From the relative concentrations, the equilibrium constants were calculated. **1** $K_{\text{eq}} = 1.0 \pm 0.2 = ([\text{glutathione}]^2[\text{aromatic disulfide}])/([\text{aromatic thiol}]^2[\text{glutathione disulfide}])$: ^1H NMR (500 MHz, D_2O) δ 7.516 (d, 2H, mixed disulfide), 7.474 (d, 4H, aromatic disulfide), 7.116 (d, 2H, aromatic thiol), 4.559 (dd, 1H, mixed disulfide), 4.518 (d, 1H, glutathione), 3.5 (s, 2H, mixed disulfide), 3.47 (s, 4H, aromatic disulfide), 3.44 (s, 2H, aromatic thiol), 3.26 (m, 1H, glutathione disulfide and mixed disulfide), 2.1 (m, 2H, glutathione and glutathione disulfide), 1.99 (m, 2H, mixed disulfide). **4** $K_{\text{eq}} = 0.67 \pm 0.02$: ^1H NMR (500 MHz, D_2O) δ 7.715 (m, 4H, mixed disulfide), 7.643 (d, 4H, aromatic disulfide), 7.397 (d, 2H, aromatic thiol), 3.690 (t, 1H, glutathione disulfide), 3.328 (dd, 2H, mixed disulfide), 3.257 (dd, 1H, glutathione), 2.494 (m, 2H, glutathione and glutathione disulfide), 2.299 (m, 2H, mixed disulfide), 2.120 (q, 2H, glutathione and glutathione disulfide), 1.989 (m, 2H, mixed disulfide).

Calculation of Components of Folding Redox Buffer. Six equations were set up to solve for the concentration of the five components (glutathione-GSH, glutathione disulfide-GSSG, aromatic thiol-ArSH, aromatic disulfide-ArSSAr, aromatic-glutathione mixed disulfide ArSSG, aromatic species-ArSX, glutathione species-GSX, disulfide species-RSSR, and thiol species-RSH). Two involved the mass balance of the glutathione and the aromatic groups (eqs 1 and 2), two

involved the chemical balance of disulfide and thiol (eqs 3 and 4), and two involved chemical equilibria (eqs 5 and 6).

$$[\text{GSX}] = (2 \times [\text{GSSG}]) + [\text{ArSSG}] + [\text{GSH}] \quad (1)$$

$$[\text{ArSX}] = (2 \times [\text{ArSSAr}]) + [\text{ArSSG}] + [\text{ArSH}] \quad (2)$$

$$[\text{RSSR}] = [\text{GSSG}] + [\text{ArSSG}] + [\text{ArSSAr}] \quad (3)$$

$$[\text{RSH}] = [\text{GSH}] + [\text{ArSH}] \quad (4)$$

$$K_{\text{eq1}} = [\text{GSH}]^2[\text{ArSSAr}]/[\text{ArSH}]^2[\text{GSSG}] \quad (5)$$

$$k_{\text{eq2}} = [\text{GSH}][\text{ArSSG}]/[\text{GSSG}][\text{ArSH}] \quad (6)$$

The two equilibria were the formation of aromatic disulfide and glutathione from aromatic thiol and glutathione disulfide (eq 5), and the formation of mixed disulfide and glutathione from aromatic thiol and glutathione disulfide (eq 6). The equilibrium constants at pH 6 were calculated from the pK_a of the thiol and the equilibrium constant at lower pH where the aromatic thiol was almost fully protonated. From the initial concentration of the five species and the six equations, the final concentration of the five species was determined numerically using the solver subroutine of Microsoft Excel. The equilibrium constant for the formation of aromatic disulfide at low pH where the aromatic thiol is almost fully protonated was assumed to be 1 since this is approximately the value for most monothiols. For example, the equilibrium constants for aromatic thiols **1** and **4** are 1.0 ± 0.2 and 0.67 ± 0.02 , respectively. The equilibrium constant for the formation of mixed disulfides at low pH was therefore assumed to be 2. Minor variations in the equilibrium constants did not appreciably affect the equilibrium concentrations of glutathione or aromatic thiol.

p-Mercaptobenzenesulfonic Acid (**4**) (25). The thiol pK_a value was determined using UV–vis spectrophotometry, as previously described (24, 31, 32); ¹H NMR (300 MHz, D₂O) δ 7.54 (d, *J* = 7.9 Hz, 2H), 7.31 (d, *J* = 7.9 Hz, 2H); ¹³C NMR (75 MHz, CD₃OD) δ 138.85, 136.03, 128.09, 125.79; mp. 99–101 °C (lit. (32) 99–101 °C).

N,N'-Dithiobis(*p*-phenylenesulfonyl)diglycine, diethyl ester. To a mixture of 4,4'-dithiobisbenzenesulfonyl chloride (25, 33, 34) (383 mg, 0.923 mmol) and glycine ethyl ester hydrochloride (362 mg, 2.59 mmol) in chloroform (8 mL) was added triethylamine (0.54 g, 5.35 mmol). After stirring of the sample for 18 h, the reaction mixture was concentrated under reduced pressure. The residue was subjected to column chromatography on silica gel (hexanes/EtOAc/CHCl₃ 4.5:4.5:1) to yield *N,N'*-[dithiobis(*p*-phenylenesulfonyl)]diglycine, diethyl ester, a white solid (400 mg, 92%). ¹H NMR (300 MHz, CDCl₃) δ 7.81 (d, *J* = 8.6 Hz, 2H), 7.59 (d, *J* = 8.6 Hz, 2H), 5.14 (brt, *J* = 5.2 Hz, 1H), 4.08 (q, *J* = 7.1 Hz, 2H), 3.78 (d, *J* = 5.3 Hz, 2H), 1.18 (t, *J* = 7.1 Hz, 3H); ¹³C NMR (125 MHz, CDCl₃) δ, 168.62, 142.19, 138.14, 128.03, 126.55, 62.04, 44.10, 13.96. Anal. Calcd for C₂₀H₂₄N₂O₈S₄: C, 43.78; H, 4.41; N, 5.11. Found C, 44.00; H, 4.21; N, 4.92.

N-[(*p*-Mercaptophenyl)sulfonyl]glycine (**5**). *N,N'*-[dithiobis(*p*-phenylenesulfonyl)]diglycine (183 mg, 0.334 mmol) was added to 1 N NaOH (5.0 mL) that had been deoxygenated by bubbling Ar through it for 15 min. The mixture was stirred under Ar for 36 h. DTT (206 mg, 1.34 mmol) was

added. After an additional 3 h, the thiol was precipitated by the addition of conc HCl (2 mL, 24 mmol). The solution was filtered, and the solid was dried under vacuum (82 mg, 50%). The thiol pK_a value was determined using UV–vis spectrophotometry, as previously described (24). ¹H NMR (300 MHz, CD₃OD) δ 7.68 (d, *J* = 8.7 Hz, 2H), 7.41 (d, *J* = 8.7 Hz, 2H), 3.68 (s, 2H); ¹³C NMR (75 MHz, CD₃OD) δ, 170.45, 139.33, 136.35, 127.56, 127.04, 43.06; HRMS [C₈H₉NO₄S₂], (*m/z*) (M⁺ + H) calcd 248.0051, found 248.0051.

S-(4-Nitrophenyl) *O*-(Phenylmethyl) Ester Carbonothioic Acid. A solution of 4-nitrobenzenethiol (23.75 g, 0.153 mol) in THF (400 mL) was cooled to 0 °C and was deoxygenated by bubbling Ar through it for 15 min. NaH (4.6 g, 0.19 mol) was added slowly over 15 min, maintaining an internal temperature below 20 °C, then CbzCl (32.5 g, 0.19 mol) was added in one portion. The mixture was placed under an Ar atmosphere and stirred at room temperature for 12 h. The residual NaH was quenched with acetone and poured onto an EtOAc/5% HCl/ice partition. The organic layer was removed and washed 2× with 5% HCl and 1× with saturated NaHCO₃, dried (MgSO₄), and concentrated. The syrup was recrystallized from 90% EtOH giving *S*-(4-nitrophenyl) *O*-(phenylmethyl) ester carbonothioic acid as a pale yellow solid (42.51 g, 96%): ¹H NMR (300 MHz, CDCl₃) δ 8.24 (d, *J* = 8.2 Hz, 2H), 7.73 (d, *J* = 8.2 Hz, 2H), 7.40 (s, 5H), 5.32 (s, 2H); ¹³C NMR (75 MHz, CDCl₃) δ 167.54, 136.30, 134.56, 128.87, 128.70, 126.32, 124.40, 123.89, 70.12; Anal. Calcd for C₁₄H₁₁NO₄S: C, 58.12; H, 3.83; N, 4.84; S, 11.08. Found C, 57.98; H, 3.75; N, 5.08, S, 11.17.

S-(4-Aminophenyl) *O*-(Phenylmethyl) Ester Carbonothioic Acid. A solution of *S*-(4-nitrophenyl) *O*-(phenylmethyl) ester carbonothioic acid (42.51 g, 0.147 mol) and SnCl₂·2H₂O (82.69 g, 0.360 mol) in EtOAc (500 mL) was refluxed for 6 h. The solution was cooled to −10 °C and NH₄OH was slowly added until a pH of 7 was attained. The tin salts were removed by filtration and the solution was washed 1× with saturated NaHCO₃, and 1× with brine, dried (MgSO₄), and concentrated. The resulting syrup was recrystallized from 70% EtOH yielding *S*-(4-aminophenyl) *O*-(phenylmethyl) ester carbonothioic acid as a pale yellow solid (38.07 g, 90%): ¹H NMR (300 MHz, CDCl₃) δ 7.38 (s, 5H), 7.30 (d, *J* = 8.2 Hz, 2H), 6.65 (d, *J* = 8.2 Hz, 2H), 5.25 (s, 2H), 3.83 (broad s, 2H); ¹³C NMR (75 MHz, CDCl₃) δ 171.10, 148.18, 136.61, 135.19, 128.55, 115.41, 114.61, 69.12; Anal. Calcd for C₁₄H₁₃NO₂S: C, 64.84; H, 5.05; N, 5.40; S, 12.37. Found C, 64.68; H, 5.33; N, 5.35; S, 12.24.

S-(4-(2-Ethoxy-2-oxoethyl)aminophenyl) *O*-(Phenylmethyl) Ester Carbonothioic Acid. A solution of *S*-(4-aminophenyl) *O*-(phenylmethyl) ester carbonothioic acid (10.00 g, 0.041 mol) and ICH₂CO₂Et (26.63 g, 0.124 mol) in DMF (20 mL) was heated to 100 °C for 30 min then cooled to room temperature. The solution was diluted with EtOAc (200 mL), then washed 2× with 5% HCl, 1× with saturated NaHCO₃ and 1× with brine, dried (MgSO₄), and concentrated. The residue was subjected to column chromatography on silica gel (hexanes/EtOAc 3:1) to give *S*-(4-(2-ethoxy-2-oxoethyl)-aminophenyl) *O*-(phenylmethyl) ester carbonothioic acid as an off-white solid (7.17 g, 51%). ¹H NMR (300 MHz, CDCl₃) δ 7.37 (s, 5H), 7.33 (d, *J* = 8.8 Hz, 2H), 6.60 (d, *J* = 8.2 Hz, 2H), 5.24 (s, 2H), 4.57 (broad t, *J* = 5.1 Hz, 1H), 4.27 (q, *J* = 7.1 Hz, 2H), 3.90 (d, *J* = 5.1 Hz, 2H), 1.32 (t,

$J = 7.1$ Hz, 3H); ^{13}C NMR (75 MHz, CDCl_3) δ 171.00, 170.53, 136.59, 128.52, 128.39, 114.26, 113.26, 69.06, 61.47, 45.29, 14.12; Anal. Calcd for $\text{C}_{18}\text{H}_{19}\text{NO}_4\text{S}$: C, 62.59; H, 5.54; N, 4.06. Found C, 62.53; H, 5.59; N, 3.89.

N-(4-Mercaptophenyl)-glycine (**6**). A suspension of *S*-(4-(2-ethoxy-2-oxoethyl)aminophenyl) *O*-(phenylmethyl) ester carbonothioic acid (1.00 g, 2.89 mmol) in 90% EtOH (20 mL) was degassed for 15 min with Ar. NaOH (1.0 g) was added and the solution was reflux under an Ar atmosphere until TLC (hexanes/EtOAc 2:1) indicated that all UV active material had an R_f value of 0. The solution was acidified with Dowex HCR-S resin, filtered and concentrated. The residue was dissolved in a minimum amount of MeOH and subjected to column chromatography on silica gel, EtOAc for 3 column volumes, followed by the elution of *N*-(4-mercaptophenyl)-glycine (0.360 g, 68%) with (EtOAc/MeOH 4:1) as a pale yellow solid: ^1H NMR (300 MHz, $\text{CD}_3\text{CO}_2\text{D}$) δ 7.22 (d, $J = 8.6$ Hz, 2H), 6.89 (d, $J = 8.8$ Hz, 2H), 4.02 (s, 2H); ^{13}C NMR (75 MHz, $\text{CD}_3\text{CO}_2\text{D}$) δ 133.17, 131.60, 116.25, 114.08, 46.87; MS [$\text{C}_8\text{H}_9\text{NO}_2\text{S}$], (m/z) ($\text{M}^- - \text{H}$) calcd 182.0, found 182.0.

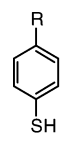
RESULTS

A series of *p*-substituted aromatic thiols, **1–5**, was selected to satisfy two criteria; the thiol pK_a values needed to range from 5 to 7 and the thiols needed to be aqueous soluble from pH 6–8 (Scheme 1). The thiol pK_a values were accurately predicted in advance using Hammett plots (24) and represent essentially the entire range of thiol pK_a values possible for mono-*p*-substituted aromatic thiols. Most proteins are folded in aqueous buffers in the pH range 6–8, and therefore all thiols needed to exhibit appreciable aqueous solubility (~ 20 mM) in this range. The aqueous solubility of aromatic thiols proved to be difficult to predict unless the R group possessed a net charge at the specific pH. Several uncharged *p*-substituted aromatic thiols were purchased or synthesized but not assayed for their protein folding capabilities due to their poor aqueous solubility ($\text{R} = \text{NH}_2$, OH, CONH_2 , SO_2NH_2 , $\text{N}(\text{CH}_2\text{CH}_2\text{OH})_2$ (35, 36)) (< 2.5 mM). Aromatic thiol **6** caused considerable protein precipitation during the protein folding reaction. The thiol pK_a value for **6** was not determined (ND) but was predicted to be 7 from Hammett plots.

Compounds **1** and **3** are commercially available, but compounds **1–4** were synthesized following literature procedures (24, 25). Compounds **5** and **6** were synthesized following published techniques (33, 34). Thiol pK_a values were obtained from the literature (**1–3**) or determined using UV-vis spectrophotometry (**4, 5**) (24, 31, 32).

The effectiveness of each thiol as a redox buffer for protein folding was determined using the protein RNase A. The protein can be obtained in several forms but most commonly either reduced RNase A and/or scrambled RNase A (sRNase A), which is oxidized RNase A with a relatively random distribution of disulfide bonds, is used (13, 14). Our previous study used both forms, and analogous results were obtained in comparable experiments (14). In using both protein forms, it was concluded that scrambled RNase A was more stable to prolonged storage than reduced RNase A; therefore, scrambled RNase A was used. The folding rates were measured based on the apparent folding rate, k^{app} , of sRNase

Scheme 1

| | | |
|--|--|---------------------|
|  | R | Thiol pK_a |
| | 1- CH_2COOH | 6.6 |
| | 2- CH_2OH | 6.4 |
| | 3- COOH | 5.95 |
| | 4- SO_3H | 5.7 |
| | 5- $\text{SO}_2\text{NHCH}_2\text{COOH}$ | 5.2 |
| | 6- NHCH_2COOH | ND |

A (**14**). The protein folding reactions were run at 25 °C, at pH 6.0 (Bis-Tris/AcOH buffer), and on a scale of 500 μL . The reactions were initiated by the addition of a concentrated sRNase A solution. Each reaction contained 0.025 mM protein, 1 mM EDTA, and 0.2 mM glutathione disulfide (GSSG). We added GSSG as it is traditionally used in the folding of disulfide containing proteins (3, 5).

The folding reactions were followed using the discontinuous assay developed by Konishi and Scheraga (28, 29) and modified as previously described (14). Aliquots were removed from the folding reaction at prescribed times, quenched in pH 5.0 buffer (Bis-Tris-AcOH buffer), and immediately assayed for RNase A activity by following the hydrolysis of 2',3'-cyclic CMP (cCMP) at 292 nm. The enzymatic activity, which is indicative of native RNase A concentration, was plotted as a function of time in the protein folding reaction and fit to $y = A(1 - e^{-kt})$, where k is the apparent folding rate constant (k^{app}), A is the maximum % folded, and t is time.

At pH 5.0, the pH used to determine the enzymatic activity, thiols **3**, **4**, and **5** (thiol pK_a values of 5.95, 5.7, and 5.2, respectively) exhibited appreciable absorbance at the assay wavelength (292 nm). At high thiol concentrations, the background absorbance of the thiolate (> 2.0) precluded the measurement of enzyme activity. The background absorbance is mainly due to the deprotonated thiolate form of the thiol. To minimize the background absorbance, a 25 mM excess of 2-aminoethyl methanethiosulfonate (AEMTS) was added to the enzymatic assay. The thiolates react rapidly with AEMTS to form mixed disulfides, which have lower extinction coefficients at 292 nm than the thiolates, thus decreasing the background absorbance of the assay. AEMTS was a reagent used extensively by Scheraga et al. to quench the folding of RNase A (28) and in control experiments had no effect on the measured enzymatic activity.

Protein folding rates in the presence of each of the five aromatic thiols and GSH at pH 6.0 were measured (Figure 2). The concentration of each thiol was varied to ascertain its optimum folding concentration, defined as the concentration at which Ak was maximized. The value of Ak corresponds to the initial rate of protein folding. The folding rate, k^{app} , at the optimal folding conditions was always within 7% of the maximum folding rate for a given thiol. For a number of the thiols, at high thiol concentrations, a precipitate was observed, and this may be responsible for the decrease in the A values.

The rapid equilibrium between the aromatic thiol and GSSG in the protein folding mixture will result in the formation of three additional species: aromatic disulfide, mixed aromatic-glutathione disulfide, and glutathione. The concentration of the five species at equilibrium can be calculated based on the initial conditions, the pH of the solution, the pK_a of the thiol, and the equilibrium constant for the formation of aromatic disulfide and glutathione from

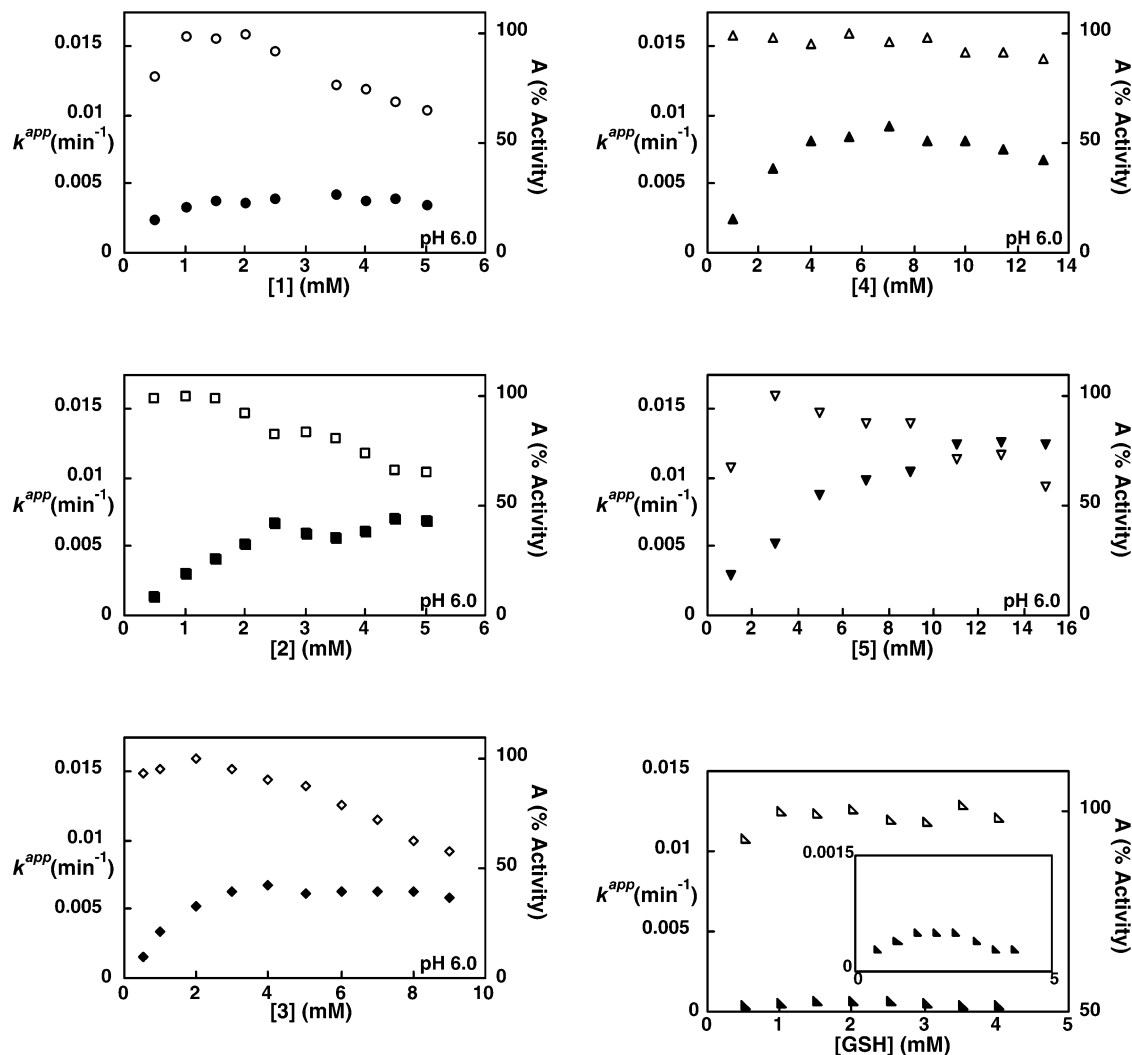


FIGURE 2: Apparent rate constant, k^{app} (closed symbols, left y axis), and maximum % activity, A (open symbols, right y axis), for the folding of scrambled RNase A versus increasing concentrations of aromatic thiols **1**–**5** and GSH; **1** (circles), **2** (squares), **3** (diamonds), **4** (point up triangles), **5** (point down triangles), and GSH (right triangles, plot in plot is k with the axis 10 \times). The apparent rate constant k for GSH is almost at the baseline. Assays were performed at pH 6.0 and 25 °C in the presence of 0.2 mM GSSG and 1 mM EDTA. Maximum % activity, A , was normalized to 100% for each compound. The A values in Table 1 have not been normalized.

glutathione disulfide and aromatic thiol at low pH where both glutathione and aromatic thiol have almost fully protonated thiol groups. At low pH, the overall equilibrium constant between glutathione disulfide and most monothiols is close to 1 (37). We have measured the equilibrium constants for compounds **1** and **4** at low pH, 1.0 and 0.7, respectively, and assume a value of 1 in all our calculations. The equilibrium constant for the formation of mixed disulfide from glutathione disulfide and aromatic thiol is thus assumed to be 2 due to statistical factors. Varying the overall K_{eq} by a factor of 2 minimally alters our calculated concentrations of glutathione or aromatic thiol, 5 and 0.7%, respectively. Because K_{eq} is assumed to be 1 for all aromatic thiols, the calculated concentrations of the individual species, with the exception of the aromatic thiolate, will be the same for all five thiols as a function of protonated aromatic thiol in solution concentration, Figure 3.

It was observed that a relationship existed for the five aromatic thiols investigated. Although the optimal concentration of each thiol differed, the concentration of the protonated aromatic form (SH form) at the optimal concentration was approximately the same. Optimal folding conditions for each

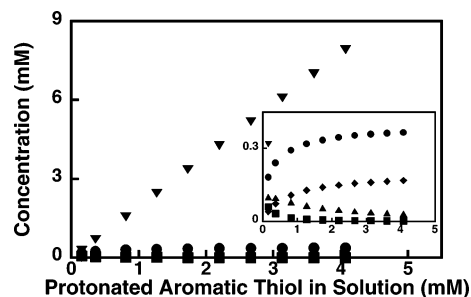


FIGURE 3: Concentrations of the five species present in the redox buffer for thiol **3** versus protonated aromatic thiol in solution (plot in plot is identical with the y axis 20 \times). The five species are glutathione (GSH, circles), glutathione disulfide (GSSG, squares), aromatic disulfide (ArSSAr, diamonds), glutathione-aromatic thiol mixed disulfide (ArSSG, triangle), and aromatic thiolate (ArS[−], inverted triangle).

of the five thiols were found to correspond to between 1.5 and 2.2 mM of aromatic thiol in the protonated form (Figure 4) and between 1.9 and 2.6 mM total protonated thiol ([GSH] + [ArSH]). At a concentration of 1.8 mM protonated aromatic thiol in solution and a total protonated thiol

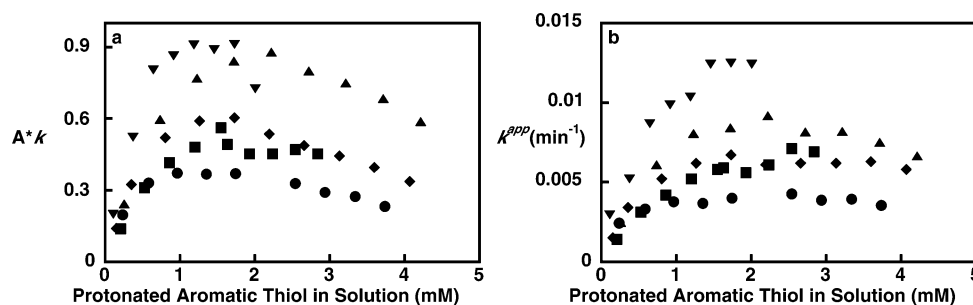


FIGURE 4: (a) $A \cdot k$ versus concentration of protonated thiol in solution. (b) Apparent rate constant, k , for the folding of scrambled RNase A versus concentration of protonated aromatic thiol in solution: 1 (circles), 2 (squares), 3 (diamonds), 4 (point up triangles), and 5 (point down triangles).

Table 1: Folding of Scrambled RNase A at pH 6.0^a

| additive | initial [ArSH] (mM) | calculated protonated thiol at equilibrium (mM) | | A (%) | $k^{app} \times 10^3$ (min ⁻¹) | relative rate |
|----------|------------------------|--|-------|---------|---|---------------|
| | | [ArSH] | [GSH] | | | |
| 1 | 2.6 | 1.8 | 0.34 | 88 ± 12 | 5.2 ± 0.4 | 0.42 ± 0.01 |
| 2 | 2.9 | 1.8 | 0.34 | 83 ± 10 | 7.5 ± 0.4 | 0.61 ± 0.06 |
| 3 | 4.2 | 1.8 | 0.34 | 91 ± 9 | 8.0 ± 0.6 | 0.64 ± 0.11 |
| 4 | 5.7 | 1.8 | 0.34 | 98 ± 9 | 9.1 ± 0.8 | 0.73 ± 0.07 |
| 5 | 13.5 | 1.8 | 0.34 | 86 ± 10 | 12.4 ± 0.8 | 1.0 |

^a The error corresponds to the 95% confidence interval, $ts/N^{0.5}$ where N is the number of data points, s is the standard deviation, and t is from the t -test table. The error was determined from four side-by-side runs comparing all five thiols.

concentration of 2.1 mM, the folding activities for each of the five thiols were compared side by side (simultaneously) four times (Table 1). The mean of A , k , and the relative rate are reported in Table 1. The A values in Table 1 have not been normalized.

A number of control experiments were run. To ensure that the increased folding rates were due to the action of only the thiol and not the functional groups attached to the thiol, protein folding reactions were run in the presence of analogues. These analogues included compounds such as *p*-hydroxyphenylacetic acid and *p*-hydroxybenzyl alcohol in which the thiol group is replaced with a hydroxyl group. The addition of an analogue to a protein folding reaction containing glutathione (GSH) and glutathione disulfide (GSSG) did not increase the apparent folding rate. In the presence of the analogue and in the absence of GSH and GSSG, no measurable folding rate was observed. Therefore, it is assumed that any folding measured after the addition of aromatic thiols is due to increased rates of thiol disulfide interchange reaction and not aromatic functional group–protein interactions.

To make certain that no autofolding was occurring in the absence of redox buffer sRNase A was placed in buffer (without any redox thiol or disulfide), under standard folding and assay conditions, at pH 6.0. No increase in enzymatic activity was observed over the course of 7 days.

Traditionally glutathione disulfide is added to protein folding mixtures to improve folding. The effect of the presence and lack of different disulfide species on the folding of RNase A was investigated. At pH 7.7, the folding rates of both reduced and scrambled RNase A were unaffected, within experimental error, by the replacement of GSSG with the corresponding ArSSAr (1 or 2) (14). At pH 7.7, the folding rate of scrambled RNase A was also unaffected if no disulfide was formally added to the mixture (14). The folding of sRNase A in the absence of formally added

disulfide was not unexpected. During the preparation of the buffered aromatic thiol solutions in D₂O, a small amount of adventitious air oxidation of the thiol to disulfide was observed (~2%, 5 mM 1), although the solutions were deoxygenated and EDTA was added. At pH 6, concentration studies were performed, identical to those illustrated in Figure 2, without the formal addition of any disulfide species. No experimental difference was observed between the plots. Because no advantage was conferred by the removal or replacement of the GSSG, we used traditional conditions.

To determine the rate enhancement by aromatic thiols over the traditional additive at pH 6.0, the folding rate of sRNase A at pH 6.0 in the presence of GSH and GSSG was determined. sRNase A was folded at pH 6.0 with varying concentrations of glutathione. The optimal folding conditions were found to be 2.0 mM GSH/0.2 mM GSSG, k and A values were $k = 0.53 \times 10^{-3} \text{ min}^{-1}$ and $A = 81\%$.

DISCUSSION

To fully understand our results, it is necessary to first examine how RNase A folds. The folding of RNase A in the presence of aliphatic redox buffers, such as glutathione and dithiothreitol (DTT), has been extensively studied. In the presence of the dithiol DTT, Scheraga has proposed that unfolded RNase A, which has eight cysteine residues, quickly forms an ensemble of preequilibrium intermediates (a quasi-steady state condition).^{12,18} These preequilibrium intermediates include fully reduced (R), one disulfide (1S), two disulfide (2S), three disulfide (3S), and four disulfide (4S) species (Figure 5). The rate determining steps in the formation of native protein are the conversion of the 1S–4S preequilibrium ensemble to the two des species (3S* species), where des means the protein possesses three native disulfide bonds, and the fourth native disulfide bond is absent and specifically designated in brackets. The 3S* species are formed predominantly (95%) from other less structured 3S

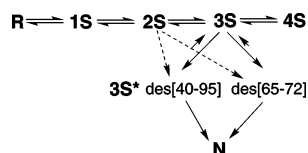
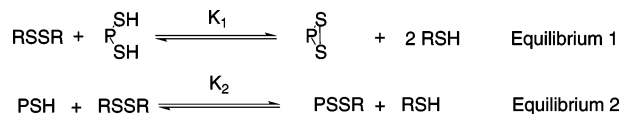


FIGURE 5: Protein folding pathway of RNase A, as proposed by Scheraga et al.^{12,18}

Scheme 2



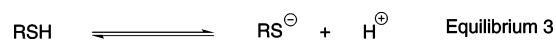
species and partially by oxidation of 2S species (Figure 5).

The folding of RNase A using the monothiol glutathione is proposed to follow a similar pattern (38–42). An ensemble of preequilibrium intermediates is quickly established, and the rate determining step is the formation of a limited number of intermediary species (S* species, comparable to the 3S*). The S* species are rapidly converted to native protein. One distinct difference between the action of DTT and glutathione is that monothiols, such as glutathione, form stable mixed disulfide species with the protein. Mixed disulfides between the protein and DTT almost always have a fleeting existence. Due to the formation of stable mixed disulfides, the regeneration of native protein with glutathione is proposed to proceed through a greater number of pathways. The basic folding pattern, however, is still the same; a preequilibrium mixture is formed and the rate determining step is conversion of the preequilibrium mixture to S* species. The similarity between the folding rates of scrambled RNase A and reduced RNase A under a wide variety of conditions, pH 7.0 or 7.7 with glutathione or with aromatic thiol **1** (14), suggests that scrambled RNase A follows a similar folding pathway.

The overall protein folding rate will be a function of the concentration of species that can be directly converted to S* species, productive intermediates, and the rate at which they are converted to S* species. The concentration of productive intermediates will be dependent upon the composition of the redox buffer. For example, at high thiol concentrations the formation of disulfide bonds will be inhibited. As a result, at high glutathione concentrations folding rates of RNase A decrease even though the rates of many of the reactions involved actually increase. Therefore, increasing the rate of the thiol-disulfide interchange reactions is very desirable but may not result in an overall increased rate of protein folding due to changes in the composition of the preequilibrium mixture.

The folding of RNase A can be evaluated in two different but related manners: the content of the preequilibrium mixture and the kinetics of protein folding. Initially issues related to the preequilibrium mixture will be discussed, and then kinetic issues will be addressed. The contents of the preequilibrium mixture will be in quasi-equilibrium with the redox buffer and thus affected by the concentration of small molecule thiol (RSH) and disulfide (RSSR) in solution (40, 42, 43). As previously proposed by others the two important equilibria between the protein and the redox buffer are those illustrated in Scheme 2, where both equilibria involve a protein thiol (PSH), a redox buffer thiol (RSH), and a redox

Scheme 3



buffer disulfide (RSSR). Equilibrium 1 is the formation of a protein disulfide (PSSP) and equilibrium 2 is the formation of a mixed disulfide (PSSR). The equilibrium constant for both of these reactions depends on the concentration of thiol in the protonated form (SH), eqs 7 and 8, and the value of the equilibrium constant will be similar for all monothiols barring any selective protein small molecule interactions. The equilibrium constant between monothiols and glutathione disulfide is close to 1 under conditions where both monothiol and glutathione have protonated thiol groups (37). Therefore, the content of the preequilibrium mixture is predicted to be similar for a given concentration of protonated thiol. If this were indeed the case one would expect a plot of k^{app} versus protonated thiol concentration for each thiol to be proportional to each other.

$$K_1 = [\text{PSSP}][\text{RSH}]^2/[\text{RSSR}][\text{P}(\text{SH})_2] \quad (7)$$

$$K_2 = [\text{PSSR}][\text{RSH}]/[\text{RSSR}][\text{PSH}] \quad (8)$$

The hypothesis that the concentration of protonated thiol in solution is important is one that has not been investigated previously. To understand the effect of protonated thiol concentration on protein folding, a series of monothiols with varying thiol pK_a values need to be examined for their ability to fold proteins. In addition, the thiol pK_a values need to vary enough to observe an effect while also staying close enough to the pH of the solution to maintain a substantial concentration of protonated thiol (Schemes 2 and 3). Given the limited number of monothiols examined previously this has not been possible. With our series of aromatic thiols, this hypothesis was tested.

Observing protein folding at pH 6.0 with our five monothiols allowed us to look at two thiols with pK_a values lower than the solution pH, two thiols with pK_a values greater than the solution pH and one nearly equal to the pH of the solution. When the values of Ak (Figure 6a) and k (Figure 6b) are plotted versus the concentration of protonated aromatic thiol at pH 6.0 similar graphs are obtained for each thiol after normalization, demonstrating as predicted that these plots are proportional to each other. The value of Ak corresponds to the initial rate of protein folding. Plots of thiolate concentration or total thiol concentration (protonated thiol + thiolate, Figure 2) versus k^{app} do not show the same similarity. For each individual thiol, the thiolate concentration is directly related to the protonated thiol concentration by the pH and the pK_a, but no general proportionality exists as the pK_a value varies for each thiol. Furthermore, the optimal thiol concentration, defined as maximum Ak , occurs at approximately 2 mM (1.5–2.2 mM) protonated aromatic thiol in solution (Figure 4). However, the optimal total thiol in solution concentrations ranged from 2.3 to 13.2 mM. Therefore we concluded that the optimal folding conditions occur at an equal concentration of protonated monothiol in solution, between 1.5 and 2.2 mM protonated aromatic thiol or 1.9 and 2.6 total protonated thiol ([GSH] + [ArSH]).

To accurately compare the protein folding rates of different thiols, each thiol needs to be at an equal concentration of protonated thiol in solution. The graphs of the protein folding

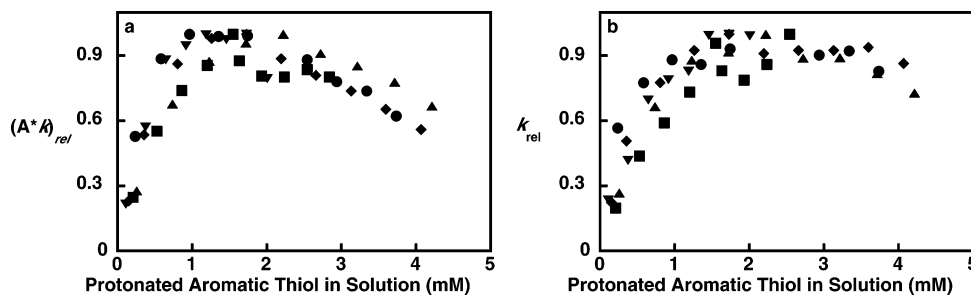


FIGURE 6: (a) $(A \cdot k)_{\text{rel}}$ versus concentration of protonated thiol in solution, where the maximum value for each compound is normalized to 1.0 (b) k_{rel} versus concentration of protonated thiol in solution, where the maximum value for each compound is normalized to 1.0. 1 (circles), 2 (squares), 3 (diamonds), 4 (point up triangles), and 5 (point down triangles).

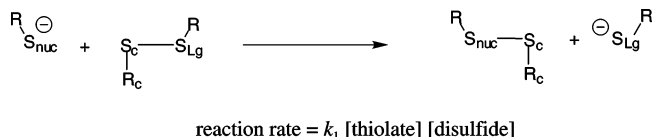


FIGURE 7: Roles of a thiol in a thiol disulfide interchange reaction. RS_{nuc} – nucleophilic thiol, RS_{c} – center thiol, RS_{lg} – leaving group thiol.

rates, k^{app} , as a function of the concentration of protonated aromatic thiol in solution adopt approximately the same shape. Therefore, at equal concentration of protonated aromatic thiol in solution the relative rates of protein folding (Figure 6b) are consistent. Our previous work compared GSH and 1 at equal protonated thiol in solution concentration at pH 7.0 but not at pH 7.7. Thus, the conclusion that the enhanced protein folding rate of aromatic thiols is due to leaving group ability needs to be reexamined, because it was obtained by comparing the results obtained at pH 7.0 to those obtained at pH 7.7.

When evaluating the kinetics of protein folding, it is important to understand the kinetics of the thiol disulfide interchange reaction. The thiol in the form of a thiolate can act as a nucleophile $\text{R-S}_{\text{nuc}}^-$, and in the form of half of a disulfide it acts as a central thiol R-S_{c} , or as the leaving group R-S_{lg} (Figure 7). As a nucleophile, the reactive form of the thiol is the thiolate; the protonated SH form is a very poor nucleophile. Therefore, the rate of reaction is dependent on the concentration of thiolate in solution. If the rate constant is expressed in terms of thiolate the rate constant k_1 will be independent of solution pH.

Thiol disulfide interchange reactions follow a Brønsted relationship (21, 22, 44), and thus the rate constant k_1 can be determined on the basis of thiol pK_{a} values. Fitting the available data to eq 9, where k_1 is the rate constant, $\text{pK}_{\text{a}}^{\text{nuc}}$ is the thiol pK_{a} value of the protonated nucleophile, $\text{pK}_{\text{a}}^{\text{c}}$ is the pK_{a} of the thiol corresponding to the central thiol being attacked, and $\text{pK}_{\text{a}}^{\text{lg}}$ is the pK_{a} of the thiol corresponding to the leaving group, Whitesides et al. determined values for the constants C , β_{nuc} , β_{c} , and β_{lg} . The values of these constants changed slightly depending on the assumptions made (eq 10); for instance, the value of β_{lg} was reported to range from -0.59 to -0.73 . The equation preferred by Whitesides et al., eq 11, assumed $\beta_{\text{lg}} = -\beta_{\text{nuc}}$, due to symmetry, and $\beta_{\text{c}} + \beta_{\text{lg}} = -1$ (21, 22, 44). In addition, if the nucleophile is an aromatic thiolate, then the value of C in eq 11 is increased by 0.9 to 7.2. However, the work of

Whitesides et al. with aromatic thiols is based on a limited data set.

$$\log k_1 = C + \beta_{\text{nuc}} \text{pK}_{\text{a}}^{\text{nuc}} + \beta_{\text{c}} \text{pK}_{\text{a}}^{\text{c}} + \beta_{\text{lg}} \text{pK}_{\text{a}}^{\text{lg}} \quad (9)$$

$$\log k_1 = (5.5 - 7.0) + (0.50 - 0.63) \text{pK}_{\text{a}}^{\text{nuc}} - (0.27 - 0.40) \text{pK}_{\text{a}}^{\text{c}} - (0.59 - 0.73) \text{pK}_{\text{a}}^{\text{lg}} \quad (10)$$

$$\log k_1 = 6.3 + 0.59 \text{pK}_{\text{a}}^{\text{nuc}} - 0.40 \text{pK}_{\text{a}}^{\text{c}} - 0.59 \text{pK}_{\text{a}}^{\text{lg}} \quad (11)$$

The values of β_{nuc} , β_{c} , and β_{lg} also can be elucidated independently. The value of β_{nuc} can be determined from a series of reactions in which the thiol is varied but the disulfide is kept constant. Under second-order conditions where $[\text{thiol}] = [\text{disulfide}]$, the intrinsic reactivity of each thiol is determined by dividing the observed second-order rate constant, k^{obs} , by the proportion of thiol in the RS^- form to generate k_1 . Under pseudo first-order conditions, $[\text{thiol}] \gg [\text{disulfide}]$, the value of k_1 also can be determined from the pseudo-first-order rate constant, k^{app} , by dividing k^{app} by the concentration of thiolate ([thiolate]). The slope of a plot of k_1 versus thiol pK_{a} is β_{nuc} . Likewise, when only the pK_{a} of the center thiol or leaving group is varied, the slope of the center thiol or leaving group pK_{a} versus k^{app} gives the value for β_{c} or β_{lg} , respectively.

The kinetic data obtained from the protein folding studies should be consistent with the major role played by the aromatic thiol in the rate determining steps. If the mode of action is predominantly nucleophilic, then the slope of a plot of $k^{\text{app}}/[\text{thiolate}]$ versus thiol pK_{a} should be consistent with the previously obtained values for β_{nuc} , 0.5 to 0.9. We have previously obtained a value of β_{nuc} for aromatic thiols of 0.9 and Whitesides obtained a range of 0.5 to 0.63. If the mode of action is predominantly leaving group, then the slope of a plot of k^{app} vs thiol pK_{a} should be consistent with values previously obtained for β_{lg} , -0.59 to -0.9 . Whitesides previously obtained a range of -0.59 to -0.73 for β_{lg} . On the basis of our β_{nuc} value of 0.9 and the assumption that $\beta_{\text{lg}} = -\beta_{\text{nuc}}$ a value of -0.9 is obtained for β_{lg} . If the mode of action is predominantly due to the center thiol then the slope of a plot of k^{app} vs thiol pK_{a} should be consistent with the β_{c} values obtained previously, -0.4 and -0.1 , by Whitesides and Hupe et al. On the basis of our β_{nuc} value of 0.9 and the assumption that $\beta_{\text{c}} + \beta_{\text{lg}} = -1$, $\beta_{\text{lg}} = -\beta_{\text{nuc}}$, we expect a $\beta_{\text{c}} = -0.1$.

To compare the protein folding data to values previously obtained for β_{nuc} , a plot of thiol pK_{a} versus $\log(k^{\text{app}}/[\text{thiolate}])$

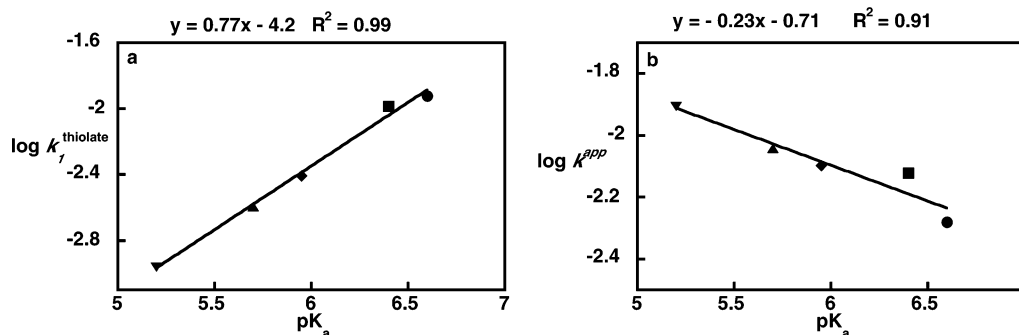


FIGURE 8: (a) $\log k_1^{\text{thiolate}}$ at 1.8 mM protonated thiol in solution versus the thiol pK_a value at pH 6.0. (b) $\log k^{\text{app}}$ at 1.8 mM, protonated thiol in solution versus thiol pK_a value at pH 6.0.

Table 2: Values of k for pH 6.0

| additive | deprotonated thiol conc [ArS ⁻] (mM) | protonated thiol conc [ArSH] (mM) | thiol pK _a | $k^{\text{app}} \times 10^3$ (min ⁻¹) | k_1^{thiolate} (mM ⁻¹ min ⁻¹) |
|----------|---|--|--------------------------|--|--|
| 1 | 0.44 | 1.8 | 6.6 | 5.2 | 12 |
| 2 | 0.73 | 1.8 | 6.4 | 7.5 | 10 |
| 3 | 2.0 | 1.8 | 5.95 | 8.0 | 3.9 |
| 4 | 3.6 | 1.8 | 5.7 | 9.1 | 2.5 |
| 5 | 11.4 | 1.8 | 5.2 | 12.4 | 1.1 |

at constant protonated aromatic thiol concentration was made ($k^{\text{app}}/[\text{thiolate}] = k_1^{\text{thiolate}}$). Since greater than 99% of glutathione, thiol pK_a = 8.7, is protonated at pH 6.0 only aromatic thiolate was taken into account. During protein folding, the concentration of thiol is much greater than that of disulfide; therefore, pseudo first-order conditions apply. In addition, the assumption is inherent that the composition of the preequilibrium mixture is similar for each thiol at a given concentration of protonated thiol in solution and a given pH (40). The assumption is consistent with the observed similarity of the folding rate versus [protonated thiol] curves and the fact that the optimal folding conditions are all obtained at similar concentrations of protonated thiol in solution. A plot of $\log k_1^{\text{thiolate}}$ versus thiol pK_a at pH 6.0 and 1.8 mM protonated thiol (Table 2) provides a slope of 0.77 ± 0.04 (Figure 8a). The value of β_{nuc} previously found (24) for aromatic thiols reacting with 2-PDE is 0.9 ± 0.1 . In addition, our results investigating the reactivity of aromatic thiols with insulin support our reported value of β_{nuc} (24). Our results with RNase A are consistent with our previously reported data.

It is also important to consider the effect that the aromatic thiol could have as a center thiol or a leaving group. The plot of k^{app} versus thiol pK_a for pH 6.0 (Figure 8b) has a slope of -0.23 ± 0.04 , which is similar to -0.1 . If the activity were due mainly to the leaving group ability, we would expect the slope to be similar to β_{lg} values obtained previously (between -0.73 and -0.59) or similar to the value computed via the equalities (-0.90). If the thiol acted both as the center thiol and the leaving group (PS⁻ attacking RSSR) in a rate determining thiol-disulfide reaction, then we would expect a slope of -1 due to the equality: $\beta_{\text{c}} + \beta_{\text{lg}} = -1$. The slope obtained from the k^{app} plot is consistent with the aromatic thiol acting as a center thiol.

The results are consistent with the aromatic thiol functioning primarily as the nucleophile and/or the center thiol, but not primarily as the leaving group, in the rate determining

steps of the major protein folding pathways. Due to the constraints on the experiment, it is not possible to distinguish between the aromatic thiol acting as a nucleophile or a center thiol. Using the equations $\beta_{\text{c}} + \beta_{\text{lg}} = -1$ and $\beta_{\text{lg}} = -\beta_{\text{nuc}}$, β_{nuc} and β_{c} are expected to differ by 1, $\beta_{\text{nuc}} - \beta_{\text{c}} = 1$. At a fixed concentration of protonated thiol, the slopes of plots for determining β_{nuc} ($\log k^{\text{app}}/[\text{thiolate}]$ vs pK_a) and β_{c} ($\log k^{\text{app}}$ vs pK_a) will also differ by approximately 1. Therefore, it is not theoretically possible to distinguish between nucleophile and/or center thiol by this method.

The rate of thiol-disulfide interchange reactions calculated for small molecule thiols with eq 5 are similar to those observed with RNase A. If we assume that the aromatic thiol is the nucleophile and that the thiols corresponding to the protein disulfide have pK_a values of 9.5, then the observed rate is 10–25% (average of 19%) of the calculated rate of protein folding. If the aromatic thiol is both the nucleophile and the center thiol and the leaving group is the protein thiol (pK_a 9.5) then the observed rate is 0.2–1.6% of the calculated rate. If the aromatic thiol is only the center thiol, then the rate cannot be calculated as it is an intramolecular reaction and eq 5 is set up for intermolecular reactions. It is not surprising that the calculated rate is higher than the observed rate, as not all species in the preequilibrium mixture can react with aromatic thiols to rapidly produce S* species, which will then rapidly produce native protein. The similarity between calculated and observed rates would imply that the reactivity of small molecule disulfides is not dramatically different from the reactivity of the disulfides contained within the folding intermediates of RNase A.

During the in vitro folding of proteins with small molecule thiol/disulfide redox buffers, there are eight general thiol disulfide interchange reactions but only six of these involve the small molecule as the nucleophile (I–IV) or center thiol (III–VI) (Figure 9) (14). Of the six reactions, only four involve a net change (I, III, V, VI) and one involves the aromatic thiol as a leaving group and center thiol (V). Thus, only three reactions (I, III, VI) are expected primarily to participate in the rate determining steps. The disulfide bond-breaking reaction in I could represent the breaking of an unstructured mixed disulfide intermediate, in preparation for the formation of a structured intermediate. Reactions III and VI can be understood as preparing a protein thiolate for an internal protein thiol disulfide interchange reaction.

Having reactions I, III, and/or VI as the major rate determining steps in the folding of RNase A is consistent with the results obtained previously for the aliphatic mono-thiol glutathione. Scheraga proposes several pathways for

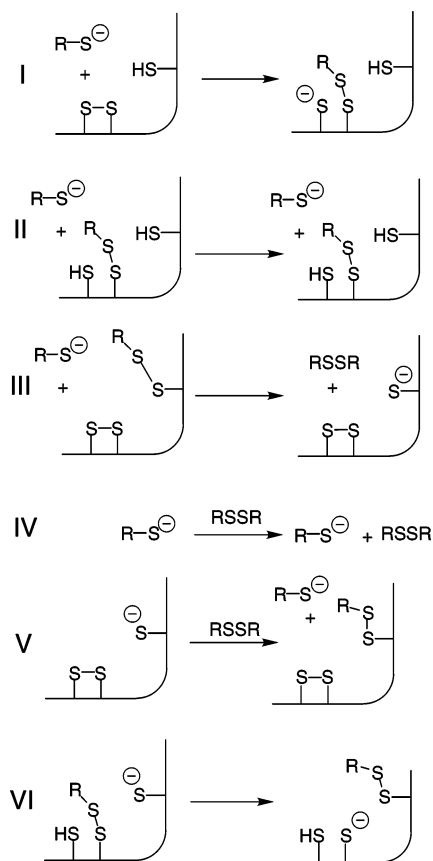


FIGURE 9: Reactions where an aromatic thiol is the nucleophile and/or center thiol in redox buffer.

the folding of RNase A with glutathione, each of which contains several possible rate determining steps (42). Reactions **I**, **III**, and/or **VI** are involved in all the major pathways.

From a practical standpoint, RNase A folds faster in the presence of aromatic thiols than glutathione. Analogous results obtained at pH 7.0 and 7.7 using reduced RNase A demonstrate that aromatic thiols are effective at folding both reduced and scrambled RNase A and that the rate enhancement over glutathione is the same for both protein forms under optimal conditions (14). It should be noted that the kinetic and preequilibrium effects play against each other. Thiols with lower pK_a values have higher folding rates at their optimal concentrations, but also higher optimal total thiol concentrations. There appears to be a competition between the concentration of reactive protein intermediates and the overall reaction rate. The most appropriate trade off between higher folding rates and higher thiol concentration will depend on the particular protein and its tolerance for a particular aromatic thiol.

In conclusion, scrambled RNase A folds faster in the presence of aromatic thiols than aliphatic thiols. At pH 6 and at optimal thiol concentrations, aromatic thiols fold sRNase A 23 times faster than glutathione. The optimal folding rate of sRNase A with aromatic thiol **5** at pH 6 was twice that observed with glutathione at pH 7.7. The optimal thiol concentration for each aromatic thiol occurs at the same concentration of protonated aromatic thiol in solution, 1.8 mM, and therefore at different total thiol concentrations. Thus, the concentration of protonated thiol in solution is more important for optimizing folding conditions than the con-

centration of thiolate. The folding rate data are consistent with the aromatic thiol acting as a nucleophile and/or a center thiol in the important rate determining steps of protein folding, but not as a leaving group. The different aromatic thiols presented show the versatility of these types of redox buffers for folding proteins under a variety of conditions.

ACKNOWLEDGMENT

We thank Dr. Michael Sponsler and Dr. Roger C. Hahn of Syracuse University for helpful comments.

REFERENCES

1. Fahey, R. C., Hunt, J. S., and Windham, G. C. (1977) *J. Mol. Evol.* 10, 155–60.
2. Thornton, J. M. (1981) *J. Mol. Biol.* 151, 261–87.
3. Rudolph, R., and Lilie, H. (1996) *FASEB J.* 10, 49–56.
4. Chaudhuri, J. B. (1994) *Ann. N. Y. Acad. Sci.* 721, 374–85.
5. De Bernardez Clark, E. (1998) *Curr. Opin. Biotechnol.* 9, 157–63.
6. Wetzel, R., Kleid, D. G., Crea, R., Heyneker, H. L., Yansura, D. G., Hirose, T., Kraszewski, A., Riggs, A. D., Itakura, K., and Goeddel, D. V. (1981) *Gene* 16, 63–71.
7. Goeddel, D. V., Kleid, D. G., Bolivar, F., Heyneker, H. L., Yansura, D. G., Crea, R., Hirose, T., Kraszewski, A., Itakura, K., and Riggs, A. D. (1979) *Proc. Natl. Acad. Sci. U.S.A.* 76, 106–10.
8. Marston, F. A. O. (1986) *Biochem. J.* 240, 1–12.
9. Marston, F. A. O., and Hartley, D. L. (1990) *Methods Enzymol.* 182, 264–76.
10. Winter, J., Lilie, H., and Rudolph, R. (2002) *FEMS Microbiol. Lett.* 213, 225–30.
11. Gilbert, H. F. (1997) *J. Biol. Chem.* 272, 29399–402.
12. Wedemeyer, W. J., Welker, E., Narayan, M., and Scheraga, H. A. (2000) *Biochemistry* 39, 4207–16.
13. Woycechowsky, K. J., Wittup, K. D., and Raines, R. T. (1999) *Chem. Biol.* 6, 871–9.
14. Gough, J. D., Williams, R. H., Jr., Donofrio, A. E., and Lees, W. J. (2002) *J. Am. Chem. Soc.* 124, 3885–92.
15. Konishi, Y., Ooi, T., and Scheraga, H. A. (1981) *Biochemistry* 20, 3945–55.
16. Darby, N. J., Morin, P. E., Talbo, G., and Creighton, T. E. (1995) *J. Mol. Biol.* 249, 463–77.
17. Weissman, J. S., and Kim, P. S. (1991) *Science* 253, 1386–93.
18. Narayan, M., Welker, E., Wedemeyer, W. J., and Scheraga, H. A. (2000) *Acc. Chem. Res.* 33, 805–12.
19. Creighton, T. E., Zapun, A., and Darby, N. J. (1995) *Trends Biotechnol.* 13, 18–23.
20. Radford, S. E., Dobson, C. M., and Evans, P. A. (1992) *Nature* 358, 302–7.
21. Wilson, J. M., Bayer, R. J., and Hupe, D. J. (1977) *J. Am. Chem. Soc.* 99, 7922–6.
22. Szajewski, R. P., and Whitesides, G. M. (1980) *J. Am. Chem. Soc.* 102, 2011–26.
23. Aultz, D. E., Helsley, G. C., Hoffman, D., McFadden, A. R., Lassman, H. B., and Wilker, J. C. (1977) *J. Med. Chem.* 20, 66–70.
24. DeCollo, T. V., and Lees, W. J. (2001) *J. Org. Chem.* 66, 4244–9.
25. Kawai, H., Sakamoto, F., Taguchi, M., Kitamura, M., Sotomura, M., and Tsukamoto, G. (1991) *Chem. Pharm. Bull.* 39, 1422–5.
26. Hawkins, H. C., Blackburn, E. C., and Freedman, R. B. (1991) *Biochem. J.* 275, 349–53.
27. Hillson, D. A., Lambert, N., and Freedman, R. B. (1984) *Methods Enzymol.* 107, 281–94.
28. Konishi, Y., and Scheraga, H. A. (1980) *Biochemistry* 19, 1308–16.
29. Crook, E. M., Mathias, A. P., and Rabin, B. R. (1960) *Biochem. J.* 74, 234–8.
30. Keire, D. A., Strauss, E., Guo, W., Noszal, B., and Rabenstein, D. L. (1992) *J. Org. Chem.* 57, 123–7.
31. Lees, W. J., Singh, R., and Whitesides, G. M. (1991) *J. Org. Chem.* 56, 7328–31.

32. Benesch, R. E., and Benesch, R. (1955) *J. Am. Chem. Soc.*, 5877–81.
33. Bubert, C., Blacker, J., Brown, S. M., Crosby, J., Fitzjohn, S., Muxworthy, J. P., Thorpe, T., and Williams, J. M. J. (2001) *Tetrahedron Lett.* 42, 4037–9.
34. Renotte, R., Sarlet, G., Thunus, L., and Lejeune, R. (2000) *Luminescence* 15, 311–20.
35. Newman, M. S., and Karnes, H. A. (1966) *J. Org. Chem.* 31, 3980–4.
36. Kaji, A., Araki, Y., and Miyazaki, K. (1971) *Bull. Chem. Soc. Jpn.* 44, 1393–9.
37. Lees, W. J., and Whitesides, G. M. (1993) *J. Org. Chem.* 58, 642–7.
38. Rothwarf, D. M., and Scheraga, H. A. (1993) *Biochemistry* 32, 2671–9.
39. Rothwarf, D. M., and Scheraga, H. A. (1993) *Biochemistry* 32, 2680–9.
40. Rothwarf, D. M., and Scheraga, H. A. (1993) *Biochemistry* 32, 2690–7.
41. Rothwarf, D. M., and Scheraga, H. A. (1993) *Biochemistry* 32, 2698–703.
42. Konishi, Y., Ooi, T., and Scheraga, H. A. (1982) *Biochemistry* 21, 4734–40.
43. Wetlaufer, D. B., Branca, P. A., and Chen, G. X. (1987) *Protein Eng.* 1, 141–6.
44. Freter, R., Pohl, E. R., Wilson, J. M., and Hupe, D. J. (1979) *J. Org. Chem.* 44, 1771–4.

BI034305C